

ADA Notice
For individuals with sensory disabilities, this document is available in alternate formats. For information call (916) 654-6410 or TDD (916) 654-3880 or write Records and Forms Management, 1120 N Street, MS-89, Sacramento, CA 95814.

1. REPORT NUMBER CA24-3924	2. GOVERNMENT ASSOCIATION NUMBER N/A	3. RECIPIENT'S CATALOG NUMBER N/A
4. TITLE AND SUBTITLE Integration of Thermal Infrared (IR) Imaging into the Caltrans Inspection Program for Pavements and Bridge Decks		5. REPORT DATE May 30, 2024
7. AUTHOR Kin S. Yen, Travis Swanston, and Ty A. Lasky		6. PERFORMING ORGANIZATION CODE AHMCT Research Center, UC Davis
9. PERFORMING ORGANIZATION NAME AND ADDRESS AHMCT Research Center UCD Dept. of Mechanical & Aerospace Engineering Davis, California 95616-5294		8. PERFORMING ORGANIZATION REPORT NO. UCD-ARR-24-05-31-01
12. SPONSORING AGENCY AND ADDRESS California Department of Transportation P.O. Box 942873, MS #83 Sacramento, CA 94273-0001		10. WORK UNIT NUMBER N/A
15. SUPPLEMENTARY NOTES N/A		11. CONTRACT OR GRANT NUMBER 65A0749 Task 3924
16. ABSTRACT The California Department of Transportation (Caltrans) must inspect pavement and bridge decks to support proactive infrastructure maintenance. By leveraging non-destructive evaluation technologies for sensing and data processing, Caltrans would improve the speed and efficiency of this critical duty. The Strategic Highway Research Program recognized the utility of Thermal IR for early identification of shallow-seated deterioration in pavements and bridge decks. Early detection allows for repair and rehabilitation ahead of significant degradation, saving time and money on maintenance. Caltrans has installed a thermal infrared (IR) system on its 3D Ground-Penetrating Radar (GPR) vehicle, allowing georeferenced visual black and white and thermal IR imaging of pavement and deck surfaces concurrent with 3D GPR imaging of the subsurface. This research continues integration of the technology within Caltrans inspection practices through identification of commercial software solutions and development of processes and procedures for acquisition of georeferenced thermal IR data; processing of data to enhance, isolate, and visualize thermal anomalies; and interpretation and presentation of results. This report documents the research effort and results.		13. TYPE OF REPORT AND PERIOD COVERED Final Report August 2021 – May 2024
17. KEY WORDS Thermal Infrared, Ground Penetrating Radar, GPR, IR, NDT, bridge deck debonding, GNSS, INS, IMU, MWIR		14. SPONSORING AGENCY CODE Caltrans
19. SECURITY CLASSIFICATION (of this report) Unclassified		18. DISTRIBUTION STATEMENT No restrictions. This document is available to the public through the National Technical Information Service, Springfield, Virginia 22161.
		20. NUMBER OF PAGES 47
		21. COST OF REPORT CHARGED N/A

Reproduction of completed page authorized

DISCLAIMER

The research reported herein was performed by the Advanced Highway Maintenance and Construction Technology (AHMCT) Research Center, within the Department of Mechanical and Aerospace Engineering at the University of California – Davis, for the Division of Research, Innovation and System Information (DRISI) at the California Department of Transportation. AHMCT and DRISI work collaboratively to complete valuable research for the California Department of Transportation.

This document is disseminated in the interest of information exchange. The contents of this report reflect the views of the authors who are responsible for the facts and accuracy of the data presented herein. The contents do not necessarily reflect the official views or policies of the State of California or the Federal Highway Administration. This publication does not constitute a standard, specification or regulation. This report does not constitute an endorsement by the Department of any product described herein.

The contents of this report do not necessarily reflect the official views or policies of the University of California. This report does not constitute an endorsement by the University of California of any product described herein.

For individuals with sensory disabilities, this document is available in alternate formats. For information, call (916) 654-8899, TTY 711, or write to California Department of Transportation, Division of Research, Innovation and System Information, MS-83, P.O. Box 942873, Sacramento, CA 94273-0001.



Advanced Highway Maintenance and Construction Technology Research Center

Department of Mechanical and Aerospace Engineering
University of California at Davis

Integration of Thermal Infrared (IR) Imaging into the Caltrans Inspection Program for Pavements and Bridge Decks

Kin S. Yen, Travis Swanston &
Ty A. Lasky: Principal Investigator

Report Number: CA24-3924
AHMCT Research Report: UCD-ARR-24-05-31-01
Final Report of Contract: 65A0749 Task 3924

May 30, 2024

California Department of Transportation

Division of Research, Innovation and System Information

Executive Summary

Problem, need, and purpose of research

The California Department of Transportation (Caltrans) must inspect pavement and bridge decks to support proactive maintenance. This need is increased by the recent Senate Bill-1 mandates. Caltrans must leverage non-destructive evaluation technologies for sensing and data processing to improve inspection speed and efficiency.

Background

Early detection allows repair and rehabilitation before significant degradation, saving time and money. In a previous project, Advanced Highway Maintenance and Construction Technology researchers worked with Caltrans to install a thermal infrared (IR) system on its 3D Ground-Penetrating Radar (GPR) vehicle. This research continued technology integration within Caltrans inspection practices through identification of commercial software solutions and development of processes and procedures for:

- Acquisition of georeferenced thermal IR data for post-processing and identification of pavement delamination and debonding.
- Processing of IR data to enhance, isolate, and visualize thermal anomalies.
- Collection and post-processing of black and white (B/W) camera pavement imagery to help positive identification of IR and GPR anomalies.

Overview of the work and methodology

The research included the following tasks:

- Identify available commercial off-the-shelf software for thermal IR data processing.
- Develop custom software to add georeferencing of data.
- Add electronics and wiring for georeferencing images from IR and B/W cameras.

Major results and recommendations

This project enabled Caltrans to start using thermal IR cameras for early identification of shallow-seated deterioration in pavements and bridge decks. The B/W imagery could help users to better identify real and false anomalies in the both 3D-GPR and IR data. As a result of this research project, Caltrans is ready to start conducting pilot projects on using the IR camera in conjunction with 3D-GPR. By completing multiple pilot projects, Caltrans personnel will gain the needed experience in data collection and analysis. Extensive real project experience is essential for developing a sound Standard Operating Procedure and recommendations for IR anomaly identification. Careful documentation of lessons learned is vital for continuing successful future deployment and maintaining institutional knowledge for the next generation of users.

Table of Contents

Executive Summary	ii
Problem, need, and purpose of research	ii
Background	ii
Overview of the work and methodology	ii
Major results and recommendations	iii
Table of Contents	iv
Figures	vi
Tables	viii
Acronyms and Abbreviations	ix
Acknowledgments	xi
Chapter 1: Introduction	1
Problem	1
Objectives and scope	1
Benefit	4
Research methodology	4
Overview of research results and benefits	4
Chapter 2: Commercial Off-the-shelf Software for Thermal IR Data Processing	5
Thermal IR software requirements	5
Web searches and literature reviews results	5
IrSUITE by Nexco	6
Nexco IrSUITE software training	7
Caltrans NDE vehicle hardware and configuration modifications for IrSUITE	7
IR camera lens calibration	8
Chapter 3: Custom Software for Georeferencing Data	10
Custom software to update IR camera geolocations	10
B/W pavement imagery camera	11
B/W camera data collection software	11
B/W imagery post-processing software	13
Chapter 4: Hardware Updates to Support Georeferencing Images from IR and B/W Cameras	25
Hardware changes	25
Ethernet switch upgrade	26
Display upgrade	26
Applanix POS sensor offsets	27

Electronics and wiring for georeferencing images from IR and B/W camera	28
Chapter 5: Deployment and Implementation	30
Problems and issues that affected product deployment and operation	30
Recommended solutions to noted problems and issues	30
Issues expected to affect full implementation	30
Other considerations for reaching full product deployment & optimal operation	31
Equipment issues	31
Operational issues	31
Policy issues	31
Chapter 6: Conclusions and Future Research	32
Future work	33
References	34

Figures

Figure 1.1: The Caltrans NDE vehicle (front and rear view). In project deployment, either the front or rear GPR antenna is used. The IR and B/W housing is mounted at the NDE vehicle rear on top of the roof.	2
Figure 1.2: Caltrans NDE vehicle camera mounts (rear view). The large white box at the top center is the IR camera housing. The smaller silver box is the B/W housing.	3
Figure 2.1: Applanix LV220 POS system COM5 port settings	8
Figure 2.2: Checkered cloth laid on the ground for IR camera rectification calibration	9
Figure 3.1: B/W camera Python application data flow diagram	11
Figure 3.2: B/W camera data collection GUI. The start and stop recording button is located at the lower right corner.	12
Figure 3.3: Applanix LV220 configuration setup view for B/W camera data collection software	12
Figure 3.4: An example B/W camera image. The gridlines are used to check georeferencing error.	13
Figure 3.5: Image on the left shows image from a fixed polarization (0°); image on the right shows image with glare reduction process applied	14
Figure 3.6: Image on the left shows image from a fixed polarization (0°); image on the right shows image with glare reduction process applied	15
Figure 3.7: An example image from the lens calibration procedure employing the use of a ChArUco checkerboard	16
Figure 3.8: Example image collected directly from the B/W camera	17
Figure 3.9: Example B/W camera images transformed to an orthographic view. There are four images overlaid on top of each other. The red text shows the image's field-of-view coverage of the ground. Lens correction was not applied here because this image was created early in the camera testing phase but was applied later.	18
Figure 3.10: Surveyed ground control points overlay on Google Earth satellite image. The mismatch of the control points positions and the Google satellite image, approximately 0.5 meter in Northing and Easting direction, are within the error margin of the satellite image accuracy.	19
Figure 3.11: Example image captured with square gridlines and ground control points. The red arrows point to the location of the ground control points.	19
Figure 3.12: Example mosaic image generated by tiling multiple orthographic camera images together from a single data recording session	20
Figure 3.13: Example overlay of mosaics from eastbound and westbound Hutchison Drive capture sessions. The result shows good alignment with the Google Earth satellite imagery as well as good run-to-run alignment. The mosaic with red outline is composed of images collected traveling	

westbound. The mosaic with blue outline is composed of images collected traveling eastbound. _____	21
Figure 3.14: Second example overlay of mosaics from eastbound and westbound Hutchison Drive capture sessions. The result shows good alignment with the Google Earth satellite imagery as well as good run-to-run alignment. The mosaic with red outline is composed of images collected traveling westbound. The mosaic with blue outline is composed of images collected traveling eastbound. _____	22
Figure 3.15: Example close-up view of orthographic mosaics illustrating minor misalignment between runs traveling in opposite directions (image on the right) and with the Google Earth imagery (image on the left). The blue line lines represent the lane marking edges detected from images traveling westbound. _____	22
Figure 3.16: Second example close-up view of orthographic mosaics illustrating minor misalignment between runs traveling in opposite directions (image on the right) and with the Google Earth imagery (image on the left). The blue line lines represent the lane marking edges detected from images traveling westbound. _____	23
Figure 3.17: Third example close-up view (without orthographic mosaics) illustrating minor misalignment between runs traveling in opposite directions and with the Google Earth imagery. The red lines represent the lane marking edges detected from images traveling eastbound, and the blue line lines represent the lane marking edges detected from images traveling westbound. _____	23
Figure 3.18: Example orthographic mosaics illustrating more noticeable longitudinal misalignment with the Google Earth imagery _____	24
Figure 4.1: Updated NDE vehicle system wiring diagram _____	25
Figure 4.2: Upgraded front vehicle display showing the vehicle trajectory and GNSS satellite availability _____	27
Figure 4.3: Wiring diagram of connections allowing the FLIR B/W camera to trigger Applanix events _____	29

Tables

Table 4.1: Serial port settings	26
Table 4.2: Applanix setting values for front 3D-GPR antenna. The Front 3D-GPR center is the reference point in this table.	27
Table 4.3: Applanix setting values for rear 3D-GPR antenna. The rear 3D-GPR center is the reference point in this table.	28

Acronyms and Abbreviations

Acronym	Definition
AHMCT	Advanced Highway Maintenance and Construction Technology Research Center
B/W	Black and White
Caltrans	California Department of Transportation
CMOS	Complementary Metal–Oxide–Semiconductor
COTS	Commercial Off–The–Shelf
CORS	Continuously Operating Reference Stations
CPR	Correct Prediction Rate
DMI	Distance Measuring Instrument
DOT	Department of Transportation
DRISI	Caltrans Division of Research, Innovation and System Information
FLIR	Forward-Looking Infrared, or Teledyne FLIR
GAMS	GNSS Azimuth Measurement System
GeoTIFF	Georeferenced Tag Image File Format
GNSS	Global navigation satellite system
GPSSGA	Global Positioning System Fixed Data
GPR	Ground-Penetrating Radar
GPS	Global Positioning System
GUI	Graphical User Interface
IMU	Inertial Measurement Unit

Acronym	Definition
IR	Infrared
MP	Megapixel
MPEG	Moving Picture Experts Group
NMEA	National Marine Electronics Association
NDE	Non-Destructive Evaluation
NDT	Non-Destructive Testing
NOAA	National Oceanic and Atmospheric Administration
OPUS	Online Positioning User Service
PDF	Portable Document Format
POS	Position and Orientation System
SB-1	Senate Bill-1
SBET	Smoothed Best Estimate of Trajectory
SDK	Software Development Kit
SOP	Standard Operating Procedure
TCP	Transmission Control Protocol
USB	Universal Serial Bus
UTC	Coordinated Universal Time

Acknowledgments

The authors thank the California Department of Transportation (Caltrans) for their support, particularly Bill Owen, Momoh Mallah, Payman Hajjani, Robert Runnestrand, and Will Dalrymple with the Geophysics and Geology Branch. The authors acknowledge the dedicated efforts of the AHMCT team who have made this work possible.

Chapter 1:

Introduction

Problem

The California Department of Transportation (Caltrans) must inspect pavement and bridge decks to support proactive infrastructure maintenance. This need is increased by recent Senate Bill-1 (SB-1) mandates. Caltrans could leverage non-destructive evaluation (NDE) technologies for sensing and data processing to improve the speed and efficiency of this critical duty.

Objectives and scope

The Strategic Highway Research Program recognized the utility of thermal infrared (IR) for early identification of shallow-seated deterioration in pavements and bridge decks. Early detection allows repair and rehabilitation before significant degradation, saving time and money. In a previous Advanced Highway Maintenance and Construction Technology (AHMCT) Research Center project, AHMCT researchers worked with Caltrans to install a thermal IR camera and a black and white (B/W) camera on its 3D Ground-Penetrating Radar (GPR) vehicle [1]. Details of the sensor and system setup are available in the final report of the previous project [1]. The system enables georeferenced visual and thermal IR imaging of pavement and deck surfaces concurrent with 3D GPR imaging of the subsurface. This research continued technology integration within Caltrans inspection practices through identification of commercial software solutions and development of processes and procedures for:

- Acquisition of georeferenced thermal IR data
- Processing of data to enhance, isolate, and visualize thermal anomalies
- Interpretation and presentation of results
- Development of software for georeferencing B/W camera imagery for pavement.



Figure 1.1: The Caltrans NDE vehicle (front and rear view). In project deployment, either the front or rear GPR antenna is used. The IR and B/W housing is mounted at the NDE vehicle rear on top of the roof.



Figure 1.2: Caltrans NDE vehicle camera mounts (rear view). The large white box at the top center is the IR camera housing. The smaller silver box is the B/W housing.

Benefit

This research enabled Caltrans to apply thermal IR technology with 3D GPR for early detection of pavement and bridge deck defects.

Research methodology

The research included the following tasks:

- Identify available commercial off-the-shelf (COTS) software for thermal IR data processing.
- Develop custom software to add georeferencing of data.
- Add electronics and wiring for georeferencing images from the IR and B/W cameras.

Overview of research results and benefits

The key deliverables of this project include:

- Identification of COTS software for thermal IR data processing, including a list of gaps in COTS software.
- Enhance the Caltrans NDE vehicle to support the installation and operation of the IR data collection software as well as georeferencing of IR camera data.
- Upgrade the Caltrans NDE vehicle hardware based on the lessons learned from these projects.
- Modify B/W camera wiring to the Applanix system to support high-accuracy georeferencing of B/W images.
- Develop and test B/W camera data collection and post-processing software.
 - Implement high-accuracy georeferencing of B/W images.
 - Implement a glare reduction process for B/W images.
 - Implement a Moving Picture Experts Group (MPEG) MP4 video exporting feature.
 - Implement perspective view to orthographic view image transformation.
 - Implement a Georeferenced Tag Image File Format (GeoTIFF) export feature.

Chapter 2:

Commercial Off-the-shelf Software for Thermal IR Data Processing

In this task, AHMCT researchers developed a list of software requirements, followed by web searches and literature reviews to identify available COTS software for thermal IR data post-processing.

Thermal IR software requirements

The following are high-level IR camera software requirements:

1. Communicate with the FLIR IR camera to start and stop recording of IR camera data via Ethernet.¹
2. Receive and store georeferencing data from the Applanix Position and Orientation System (POS) along with the IR camera data
3. Post-process the collected IR camera and location data to identify probable delamination and debonding locations.
4. COTS software is preferred in the software selection.

Web searches and literature reviews results

Web searches and literature reviews were conducted to identify available software for IR camera image and georeferencing data collection and IR image post-processing for delamination detection.

FLIR's ResearchIR software was provided by FLIR when purchasing the IR camera. ResearchIR software satisfied requirements 1 and 4, but it did not meet requirements 2 and 3. Web searches revealed that there is a MATLAB library for reading the FLIR raw files collected and stored by the ResearchIR software.

Web searches also found non-destructive testing (NDT) service providers who had developed their own in-house IR camera data collection and post-processing software. However, their software is not available for sale. These NDT service providers are:

- [Penetradar.com \(http://www.penetradar.com/infrared-thermography-\(irt\)-inspection-of-bridge-decks.html\)](http://www.penetradar.com/infrared-thermography-(irt)-inspection-of-bridge-decks.html)

¹ FLIR can be a generic acronym for forward-looking infrared. Herein, FLIR refers to the company Teledyne FLIR.

- [Infrasense.com \(https://infrasense.com/technology/infrared-thermography\)](https://infrasense.com/technology/infrared-thermography)
- [Infrared-diagnostics Inc \(https://www.infrared-diagnostics-inc.com/bridge-deck-investigation\)](https://www.infrared-diagnostics-inc.com/bridge-deck-investigation)

Working with Nebraska Department of Transportation (DOT), University of Nebraska researchers used FLIR's ResearchIR software and MATLAB to post-process the temperature data from ResearchIR in FLIR-tiff file format [2], [3]. Shen et al. developed three different methods: a grayscale morphological reconstruction method, level-set segmentation method, and deep learning method to determine delamination and debonding defect locations. They found that the level-set method has an average 80.2% correct prediction rate (CPR), and the deep learning method achieved 78% CPR. They also found that the σ (standard deviation) CPR of the deep learning method is slightly greater than the level-set method, which indicated that performance of the deep learning method was less consistent (larger variance) than the level-set method. Their research also identified challenges and pitfalls of using IR data. These challenges are:

- 1) Shadows from trees, bridge parapet walls, light poles, etc.
- 2) Dark asphalt smears on concrete decks.
- 3) Excessive dirt/gravel coverings on the deck surface.
- 4) Patches of significantly different materials/colors and textures.
- 5) Wet deck surfaces or even dry surfaces shortly after rains.

Shen et al. suggested that users' discretion and experience are needed to mitigate these real-world field survey conditions.

IrSUITE by Nexco

[Nexco-West USA, Inc. \(https://www.w-nexco-usa.com/\)](https://www.w-nexco-usa.com/) provides products and services for structural inspection as well as training on the use of NDE techniques. In Chapter 2 of a previous AHMCT research project final report, AHMCT researchers highlighted Nexco's research publications on the use of IR cameras for pavement delamination and debonding identifications using their mobile vehicle system [1]. Nexco developed IrSUITE to gather IR camera data with Global Positioning System (GPS) locations and post-process IR data to locate pavement defects. [Nexco IrSUITE flyer \(https://www.w-nexco-usa.com/assets/documents/IR%20SUITE.pdf\)](https://www.w-nexco-usa.com/assets/documents/IR%20SUITE.pdf) provides high-level detail on the software capabilities. Only Nexco IR data collection and analysis software was found to be suitable for Caltrans' specific pavement delamination detection application and the software requirements listed above. After meeting with Nexco personnel, Caltrans proceeded with IrSUITE software and training procurement based on AHMCT research results.

IrSUITE does support collecting additional pavement surface B/W imagery from a line scan camera. However, the supported line scan camera is no longer being manufactured. Nexco has enhanced IrSUITE software to support additional line scan cameras currently being manufactured. However, the supported line scan camera was not available due to supply chain constraints. Additional line scan camera options became available late in the research timeline and are now available, but these could not be evaluated due to time and budget constraints. As a result, a different custom B/W camera system was installed to support pavement imagery collection. Details of the B/W camera system are provided in Chapters 3 and 4.

Nexco IrSUITE software training

Caltrans purchased a three-day IrSUITE training. The IrSUITE training was conducted from March 7 to March 10, 2022 at an AHMCT research facility. The training covered software setup, data collection, data analysis, and post-processing. An IrSUITE manual in Portable Document Format (PDF) format was provided.

Caltrans NDE vehicle hardware and configuration modifications for IrSUITE

IrSUITE requires real-time GPS positions during data collection in order to georeference the IR image data. In early email pre-purchase communications, Nexco indicated that IrSUITE's preferred GPS position data stream is the National Marine Electronics Association (NMEA) Global Positioning System Fixed Data (GPGGA) messages at 20 Hz via a serial port. A USB-to-serial (RS232) adapter was added to the Caltrans NDE vehicle computer to provide the necessary communications. The Universal Serial Bus (USB) port of the USB-to-serial adapter is connected to the NDE vehicle computer, and the RS232 serial port of the USB-to-serial adapter is connected to the Applanix LV220 POS computer COM5 port. The RS232 baud rate for both computer and Applanix COM4 was set to 19200 bits per second. Working with the Nexco representative at the time of the IrSuite training and installation of the software on the NDE vehicle system, the final NMEA GPGGA message output rate was set to 10 Hz on the Applanix LV220 POS system COM5 port.

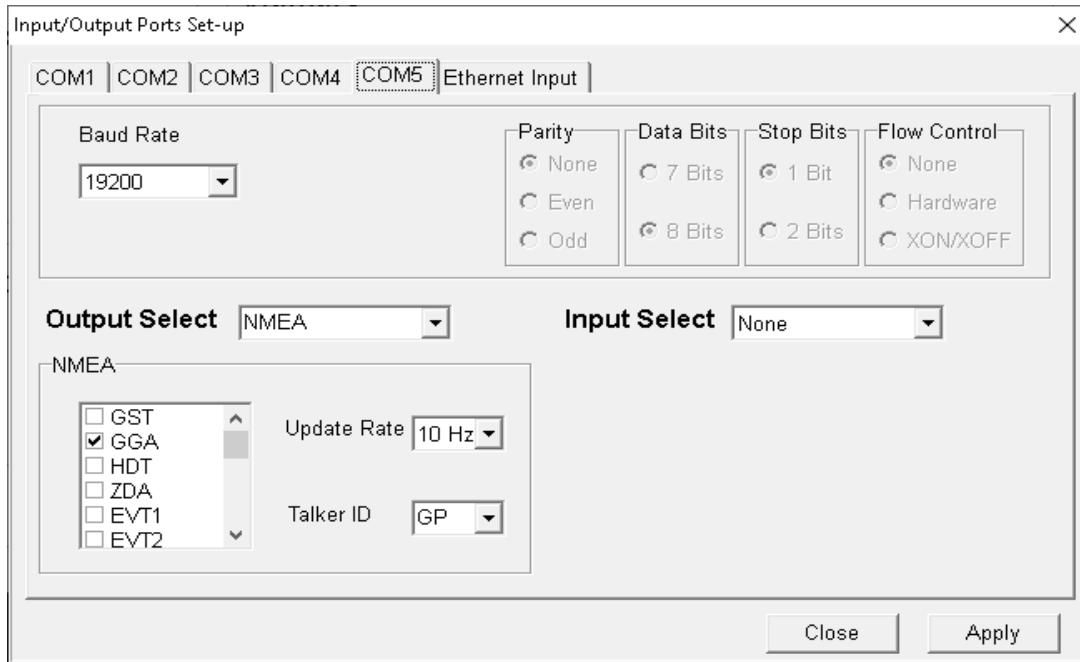


Figure 2.1: Applanix LV220 POS system COM5 port settings

IR camera lens calibration

IrSUITE has functions and procedures to calibrate the IR camera lens to provide accurate rectification of pavement IR imagery. Nexco recommends any checkerboard patten less than 12 ft in length and width with a consistent and accurate checkerboard patten. A few checkerboard photography backdrops and checkerboard tablecloths were purchased from [Amazon](https://www.amazon.com/) (<https://www.amazon.com/>). Figure 2.2 shows the checkerboard backdrop selected for IR camera calibration. Its dimensions are 102 inches x 60 inches. The checker size is 3.74 inches x 3.74 inches square. Alternatively, a custom checkerboard patten can be printed using a large-format printer at a higher cost.

To facilitate IR camera calibration, a removable 1080p portable monitor is temporarily added to the rear of the NDE vehicle. The users can easily see the IR camera image output and position the calibration checkerboard in the IR camera's field of view center using the rear monitor. The portable monitor is then stowed away for safe storage after the calibration process.



Figure 2.2: Checkered cloth laid on the ground for IR camera rectification calibration

Chapter 3:

Custom Software for Georeferencing Data

Custom software to update IR camera geolocations

The Caltrans NDE vehicle uses an Applanix LV220 POS system to provide real-time position and orientation data via serial RS232 ports and Ethernet interface to all the on-board sensors, such as cameras and a GPR computer. However, the real-time position accuracy is only about 0.5 to 5 meters.

To obtain high-accuracy (centimeter-level) position and orientation data, Caltrans post-processes the Applanix LV220 POS raw data (Global Navigation Satellite System [GNSS], Inertial Measurement Unit [IMU] and Distance Measuring Instrument [DMI]) with GNSS base station(s) data. The GNSS base station data can come from National Oceanic and Atmospheric Administration (NOAA) National Geodetic Survey Continuously Operating Reference Stations (CORS), Caltrans GNSS network, or a temporary static GNSS base station set up locally. Applanix POSPac MMS software is used to post-process Applanix POS raw data. The post-processed solution data can be exported to NMEA GPGGA messages in text format or other data formats up to 100 Hz. Caltrans personnel generally export post-processed position solutions in the NMEA message text format to update the 3D GPR data position data. The GPR post-processing software, Examiner, can import the exported NMEA message text file to update the 3D GPR position data.

The Nexco IrSUITE software logs the IR camera position data in a text file with NMEA GPGGA-formatted messages. IrSUITE does not have a feature that imports post-processed position data to update its existing log file position data. AHMCT researchers developed custom Python software to update the position data into the IrSUITE position log file. The Python software uses Coordinated Universal Time (UTC) in the IrSUITE log file to find the corresponding position at the same UTC time in the exported NMEA GPGGA message text file. Then, the software overwrites the position data in the IrSUITE position log file with the post-processed positions.

B/W pavement imagery camera

Nexco's line scan camera was not a viable option for Caltrans pavement imagery due to camera availability and cost. The pavement imagery data are needed to better identify anomalies during 3D-GPR post-processing. In addition, the pavement images are also used to help in delamination and debonding detection in IR camera image post-processing.

A FLIR Blackfly S BFS-U3-51S5P-C camera body with a Fujinon HF12XA-5M 12.4 mm lens was installed to collect B/W pavement imagery. AHMCT researchers developed Python-based software applications for both data collection and image post-processing. The B/W image post-processing software performs glare reduction and orthographic projection correction on the B/W images. It also outputs MP4 videos and orthographic GeoTIFF images.

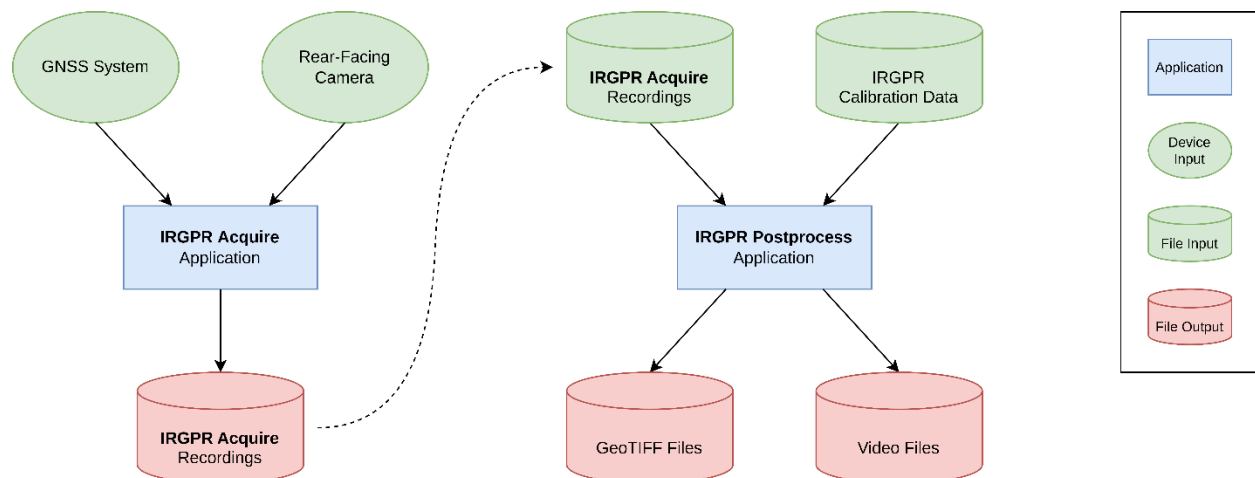


Figure 3.1: B/W camera Python application data flow diagram

B/W camera data collection software

The B/W camera data collection software provides the user with a Graphical User Interface (GUI) to control the camera frame rate and to start and stop the data recording. Figure 3.2 shows the B/W camera data collection GUI. The GUI also provides a real-time camera image view as well as operational status data such as GNSS position, speed, and number of image frames collected.

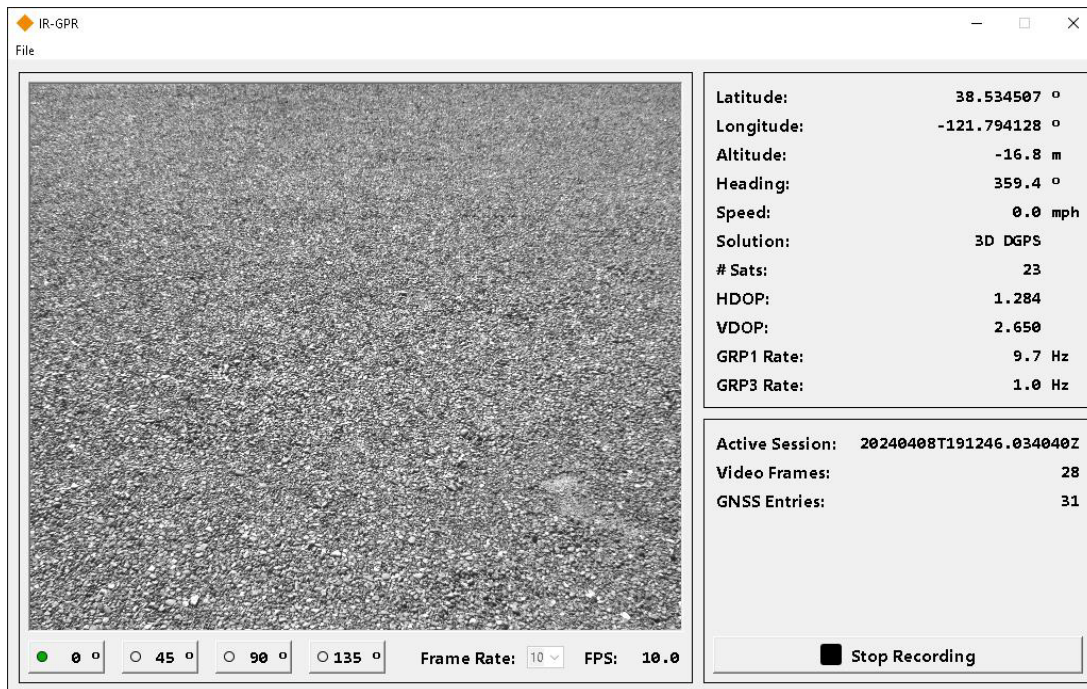


Figure 3.2: B/W camera data collection GUI. The start and stop recording button is located at the lower right corner.

The B/W camera data collection software communicates with the FLIR Blackfly S camera via the computer USB 3 interface. It also receives the position data from the Applanix LV220 POS via the computer Ethernet interface. Figure 3.3 shows the Applanix LV220 configuration setup to support the B/W camera data collection software. Group 1 and 3 messages are enabled, and the Group 1 output rate is set to 10 Hz using Transmission Control Protocol (TCP).

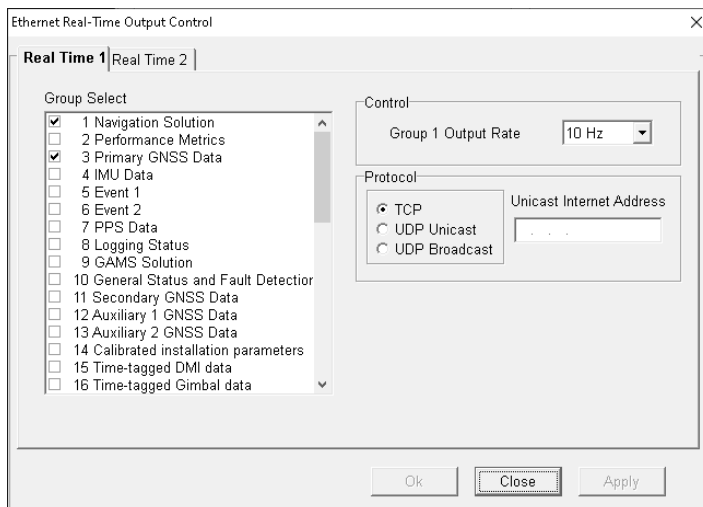


Figure 3.3: Applanix LV220 configuration setup view for B/W camera data collection software

Each B/W camera data collection session data set, from single start and stop data recording session, is stored in an individual folder named using the UTC time of the start of the data recording session. An example folder name is 20230722T184259.368796Z. The first eight digits of the folder name show the year, month, and date. The images are stored in uncompressed raw format in a single file.

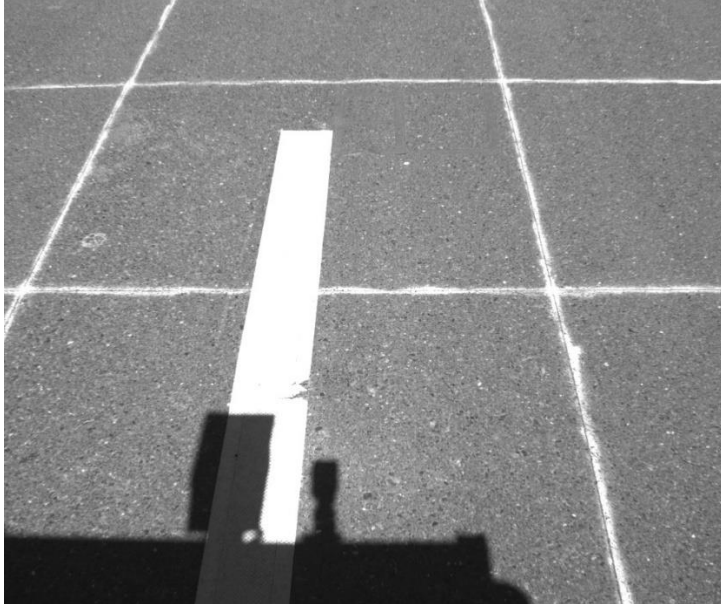


Figure 3.4: An example B/W camera image. The gridlines are used to check georeferencing error.

B/W imagery post-processing software

Anti-glare polarized pixel output

Outdoor lighting conditions can present challenges to collecting good pavement images with traditional cameras. Glare and reflections from strong sunlight can adversely affect pavement image quality. Some FLIR machine vision cameras use Sony's on-sensor polarization and anti-glare features that promise to improve image quality in challenging lighting situations. The on-sensor polarization image sensors on these cameras are composed of individual pixels, each with its own polarizing filters oriented to 0°, 45°, 90° and 135°. The polarized pixels are arranged in repeating pixel blocks. Sony's IMX253MZR and IMX250MZR sensors have this on-sensor polarization feature and are based on their twelve and five-megapixel IMX253 and IMX250 global shutter complementary metal-oxide-semiconductor (CMOS) sensors.

The FLIR Blackfly S BFS-U3-51S5P-C has a 5.0-megapixel (MP) Sony IMX250MZR CMOS image sensor. The four sets of polarized images enable users to compensate for changing lighting conditions, such as glare, reflection, and the

relative movement and orientation of the vehicle. The FLIR Blackfly S BFS-U3-51S5P-C camera was installed on the Caltrans NDE vehicle to collect pavement images. Detailed specifications of the [FLIR Blackfly S BFS-U3-51S5P-C camera](https://www.flir.com/products/blackfly-s-usb3/?model=BFS-U3-51S5P-C) (<https://www.flir.com/products/blackfly-s-usb3/?model=BFS-U3-51S5P-C>) are available on FLIR's website.

The disadvantage of image sensors with on-sensor polarization is lower image resolution, higher cost, and a limited selection of cameras. However, these sensors can improve pavement imagery, particularly when the sun is low on the horizon and presents strong glare on pavement images.

Our glare reduction process mimics the approach implemented by the `CreateGlareReduced()` function in the `ImageUtilityPolarization` class of FLIR's [Spinnaker Software Development Kit \(SDK\)](http://softwareservices.flir.com/Spinnaker/latest/class_spinnaker_1_1_image_utility_polarization.html#a3c4a8bee7fb5ebf4bb9c0ec2bc39e329) (http://softwareservices.flir.com/Spinnaker/latest/class_spinnaker_1_1_image_utility_polarization.html#a3c4a8bee7fb5ebf4bb9c0ec2bc39e329). The glare-reduced image is produced by selecting, for each pixel, the darkest value of the four polarizations (0° , 45° , 90° , and 135°) for that pixel. The algorithm is implemented in Python with code developed by AHMCT researchers instead of using the Spinnaker SDK to reduce software complexity and dependencies. Figures 3.5 and 3.6 shows examples of images before and after the glare reduction process. The images in the figures were collected late afternoon at 5 to 6 pm with the sun low on the horizon and the vehicle traveling eastbound.

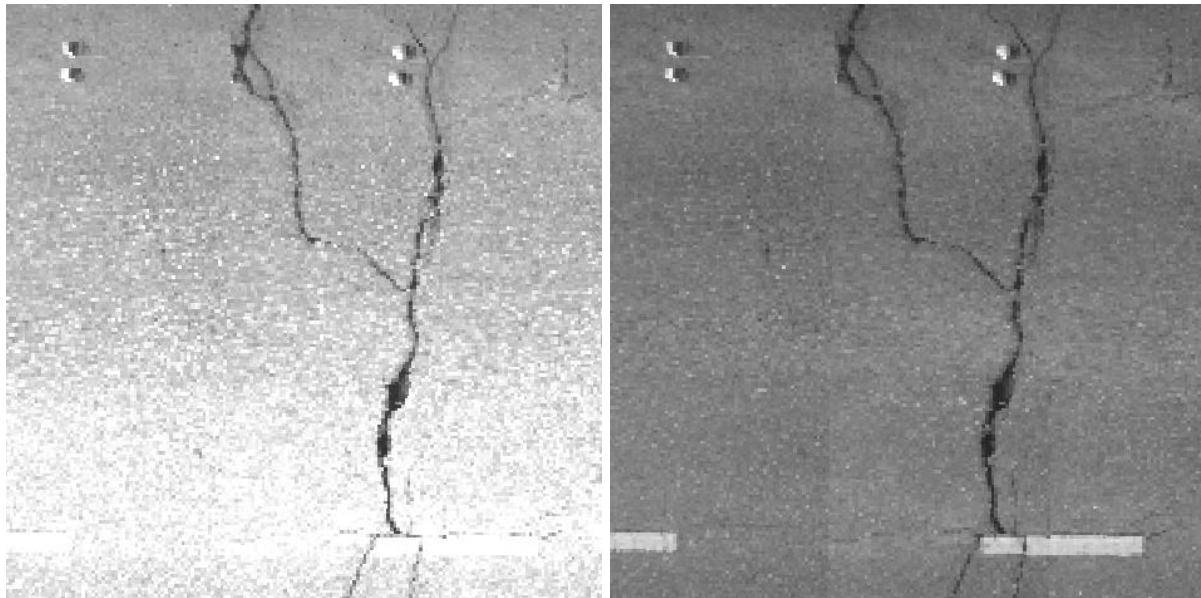


Figure 3.5: Image on the left shows image from a fixed polarization (0°); image on the right shows image with glare reduction process applied

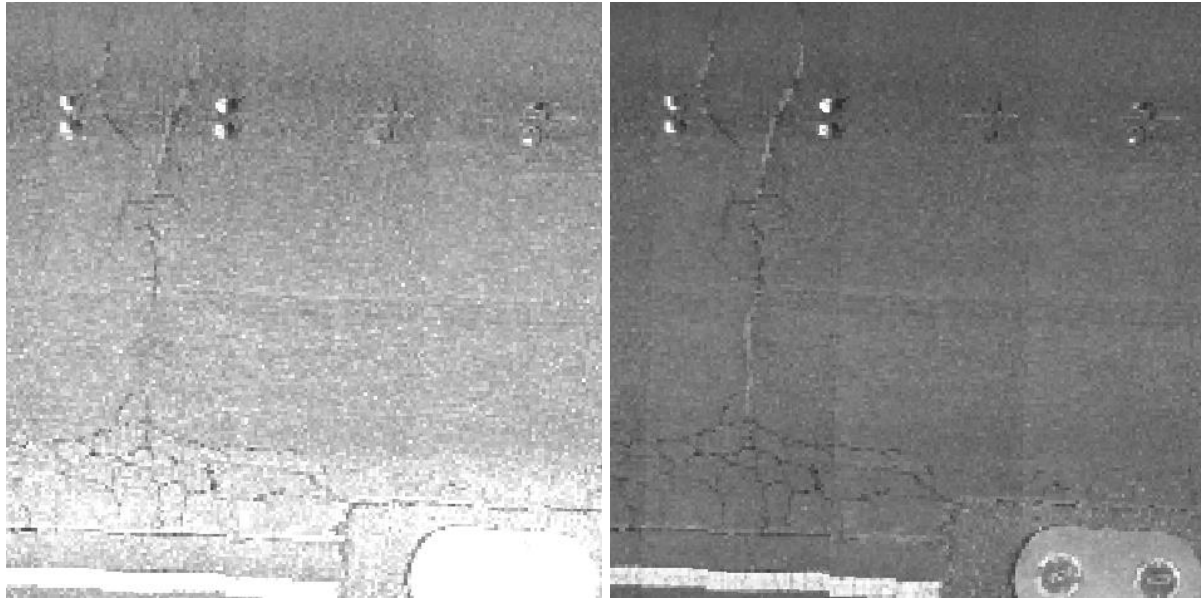


Figure 3.6: Image on the left shows image from a fixed polarization (0°); image on the right shows image with glare reduction process applied

Lens Calibration

Different camera lens and image combinations produce different distortion patterns on the image. To accurately rectify the lens distortion, we employed a well-documented lens calibration procedure from [OpenCV](https://opencv.org/) (<https://opencv.org/>) using a ChArUco checkerboard pattern. An overview of this approach can be found at [Calibration with ArUco and ChArUco](https://docs.opencv.org/4.x/da/d13/tutorial_aruco_calibration.html) (https://docs.opencv.org/4.x/da/d13/tutorial_aruco_calibration.html).

A series of images was taken with the ChArUco checkerboard in various orientations at different areas in the camera's field of view. Figure 3.7 shows an example image taken by the B/W camera during the lens calibration process. The red squares highlight the ArUco markers detected by the software. The ChArUco checkerboard was laser-printed on 11" x 17" paper and mounted onto a flat glass plate. A Python application was written by AHMCT researchers to process the collected images and through the use of various features of the open-source OpenCV library, calculate a set of lens calibration parameters.

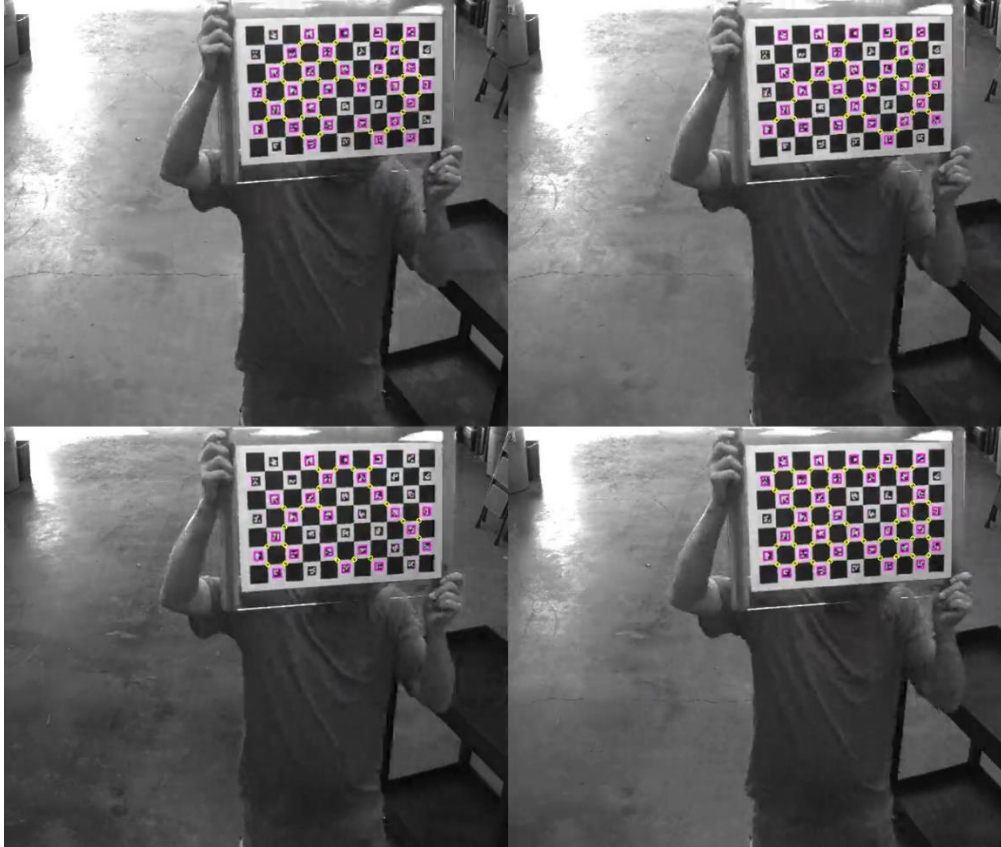


Figure 3.7: An example image from the lens calibration procedure employing the use of a ChArUco checkerboard

MP4 export

The 3D-GPR Examiner software supports the integration of MP4 videos from external cameras. Some users have employed a GoPro camera for this purpose. The user needs to provide the video's approximate starting location and its frame rate to the Examiner software; Examiner will then be able to synchronize the video view with the 3D-GPR data view.

To support 3D-GPR post-processing, the B/W image post-processing software outputs MP4 video using H.264 compression using the same frame rate at which the images were collected. The glare reduction process is applied to each frame during the video output process. The MP4 video is currently configurable at various resolutions from native 1224x1024 to 500x500. The user can also export the rectified orthographic pavement image or the non-rectified native camera view image in the MP4 video. This MP4 output process can be configured and executed by passing specific command-line parameters to the post-processing application.

Creation of orthographic B/W imagery by means of perspective transformation

One of the software requirements is to output pavement imagery that can be overlaid onto a map in either ArcGIS or Google Earth software applications. This feature enables Caltrans users statewide to view the B/W pavement imagery data alongside GPR data using software that is generally available to all Caltrans users statewide.

To meet the above requirement, the B/W perspective-view pavement imagery must be reprojected to an orthographic aerial view. Figure 3.8 shows an example B/W image from the camera without any post-processing. Figure 3.9 shows B/W camera images transformed to orthographic view.

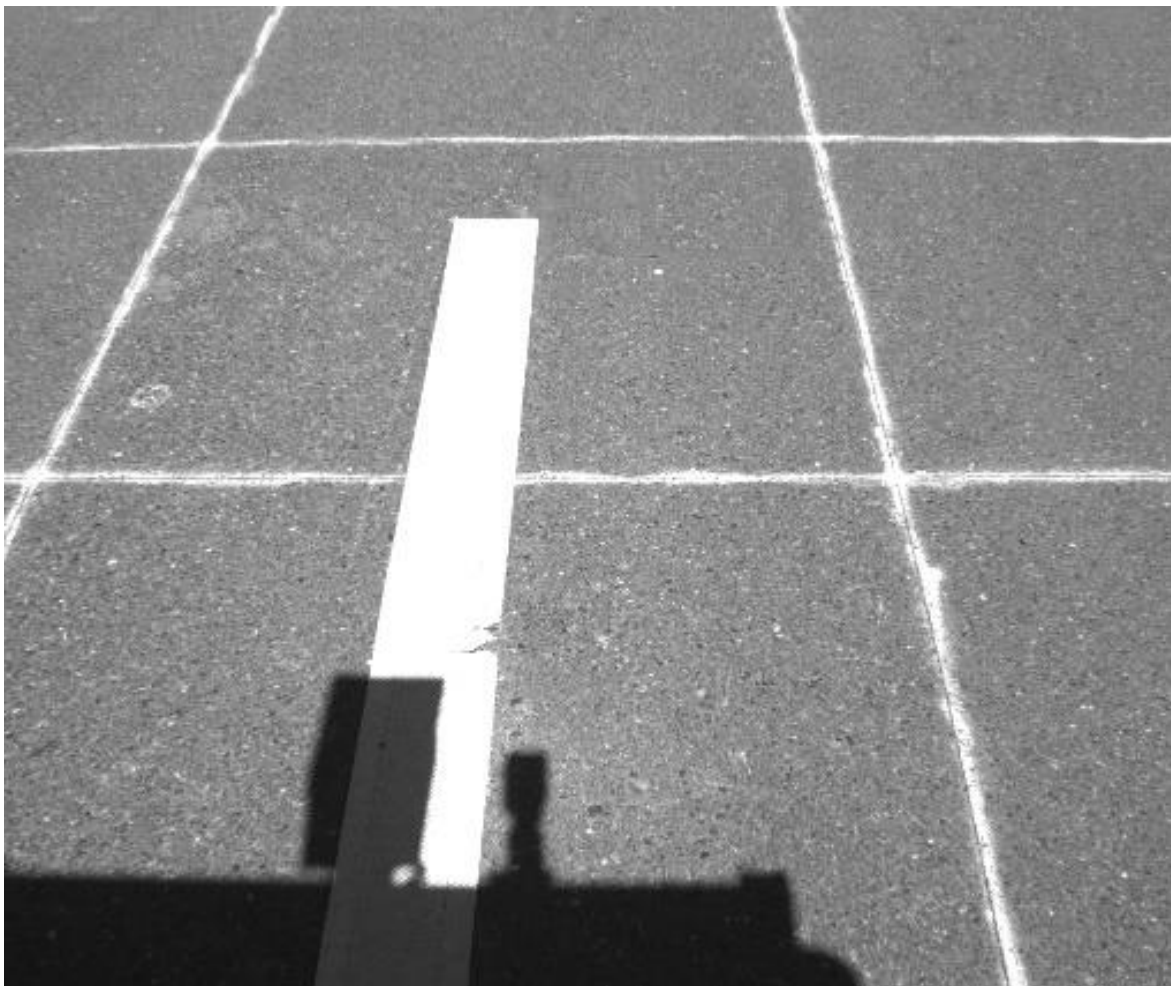


Figure 3.8: Example image collected directly from the B/W camera

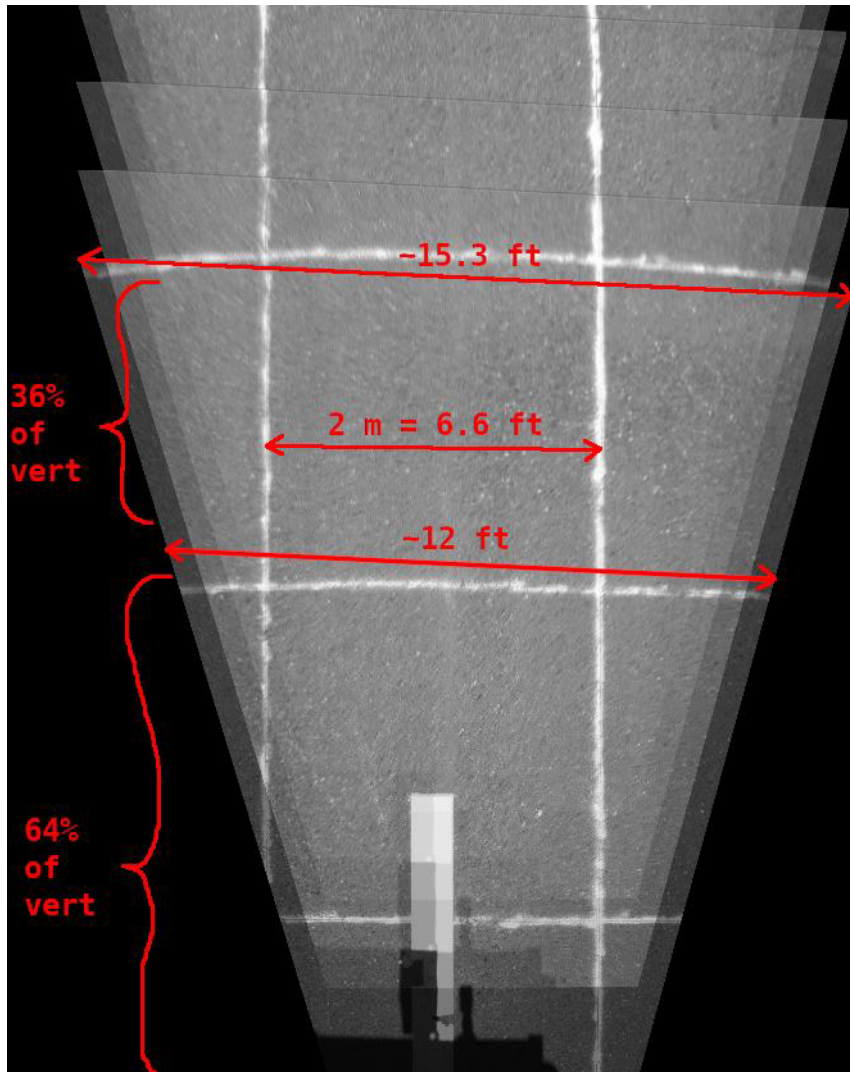


Figure 3.9: Example B/W camera images transformed to an orthographic view. There are four images overlaid on top of each other. The red text shows the image's field-of-view coverage of the ground. Lens correction was not applied here because this image was created early in the camera testing phase but was applied later.

AHMCT researchers created a set of square gridlines on the AHMCT Research Center test track as seen in Figure 3.10. The squares are 2 meters x 2 meters in size. The positions of several square corners were surveyed using a GNSS receiver collecting static data for two hours. Rapid NOAA Online Positioning User Service (OPUS) was used to post-process the GNSS static session data to calculate square corner point positions with centimeter-level accuracy. Figure 3.10 shows the surveyed point positions overlaid on a Google Earth satellite image. P1 to P6 are surveyed points and V1 to V6 are interpolated point positions based on the positions of P1 to P6. The gridlines help to show any

misalignment resulting from the orthographic transformation and provide visual confirmation of transformation accuracy.



Figure 3.10: Surveyed ground control points overlay on Google Earth satellite image. The mismatch of the control points positions and the Google satellite image, approximately 0.5 meter in Northing and Easting direction, are within the error margin of the satellite image accuracy.

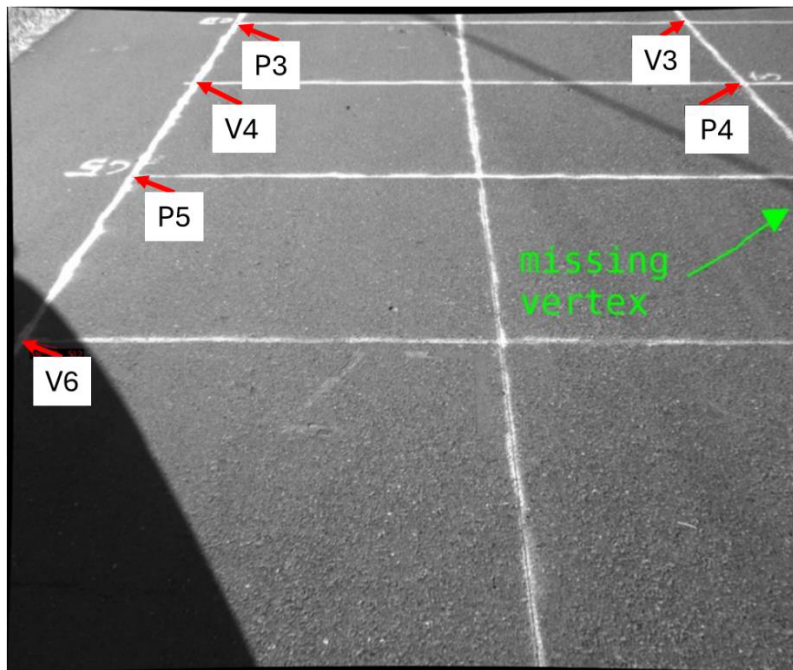


Figure 3.11: Example image captured with square gridlines and ground control points. The red arrows point to the location of the ground control points.

To calculate the perspective transformation parameters, several images of the square gride and ground control points were taken with the B/W camera with the vehicle in various positions and orientations. Figure 3.11 shows an example image captured with the square gridlines and ground control points in view. The perspective transformation parameters are then determined through

an iterative process using the collected images and vehicle position and orientation data. The perspective transformation parameters were then evaluated using a different dataset to estimate their accuracy.

Using the perspective transformation parameters, every B/W pavement image can be transformed into an orthographic image, as shown in Figure 3.12, after application of lens distortion correction and the glare reduction process. The orthographic images can then be cropped and tiled to create a mosaic GeoTIFF (see Figure 3.12) to be imported into ArcGIS or Google Earth.

The image cropping algorithm is designed to produce an optimal crop of each frame for the purpose of generating a continuous mosaic. The lateral dimension of each crop is chosen by considering the camera frame rate and the vehicle speed at the time the frame was captured. The intra-frame position of the crop is chosen such that the narrowest portion of the crop has a lateral roadway coverage that is at least as great as a (configurable) minimum-coverage value. In addition, since the imagery closer to the camera is of significantly higher quality (as it is of higher resolution and has a higher angle of incidence), the intra-frame position of the crop is also chosen such that imagery closer to the camera is preferred.

Once mosaic generation is complete, the post-processing application exports it to a file in GeoTIFF format.

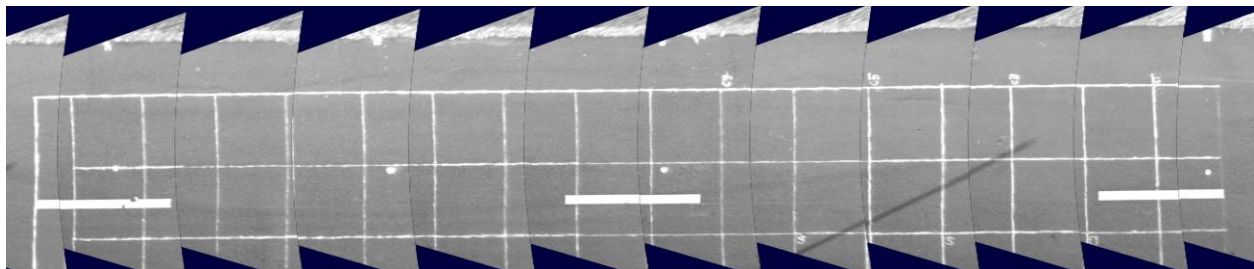


Figure 3.12: Example mosaic image generated by tiling multiple orthographic camera images together from a single data recording session

B/W camera software testing and evaluation results

The B/W camera post-processing software was tested using data collected on Hutchison Drive near the AHMCT Research Center. Hutchison Drive is an undivided rural two-lane roadway with an east-west orientation. B/W imagery was collected with the vehicle traveling both eastbound and westbound. The vehicle was driven such that there were some overlaps of the B/W imagery of the center of the roadway. The vehicle speed was about 45 mph with the camera frame rate set at 10 frames per second. The vehicle position data values were enhanced using Applanix POSPac MMS GNSS/IMU post-processing software to achieve centimeter-level accuracy.

The orthographic mosaics were overlaid onto Google Earth satellite imagery for comparison. In addition, the overlapping area of imagery from eastbound and westbound sessions were examined for any discrepancies or mismatches using features on the road surface, focusing on lateral and longitudinal misalignment of features. Paint striping, road surface cracks, and road markings were used to check for lateral and longitudinal misalignment, particularly where the road is curved.

Figures 3.13 and 3.14 show good lateral and longitudinal alignment of the mosaic image with the Google Earth satellite image and alignment between images traveling from opposite directions. Figures 3.15, 3.16, and 3.17 show close-up views of example orthographic images overlaid onto Google Earth satellite imagery. The red lines represent the lane marking edges detected from images traveling eastbound, and the blue line lines represent the lane marking edges detected from images traveling westbound. The red and blue lines illustrate minor misalignment with each other and with the Google Earth image.

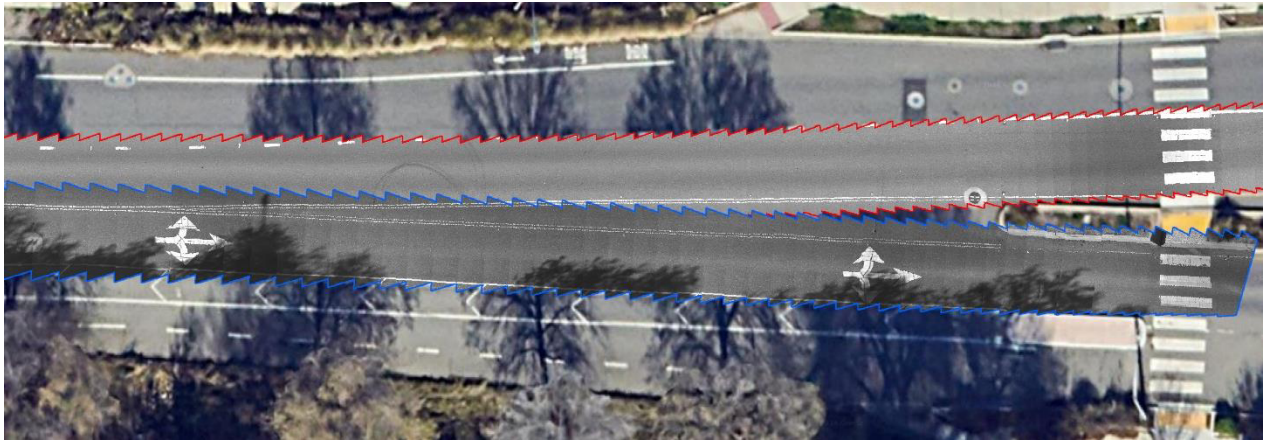


Figure 3.13: Example overlay of mosaics from eastbound and westbound Hutchison Drive capture sessions. The result shows good alignment with the Google Earth satellite imagery as well as good run-to-run alignment. The mosaic with red outline is composed of images collected traveling westbound. The mosaic with blue outline is composed of images collected traveling eastbound.



Figure 3.14: Second example overlay of mosaics from eastbound and westbound Hutchison Drive capture sessions. The result shows good alignment with the Google Earth satellite imagery as well as good run-to-run alignment. The mosaic with red outline is composed of images collected traveling westbound. The mosaic with blue outline is composed of images collected traveling eastbound.

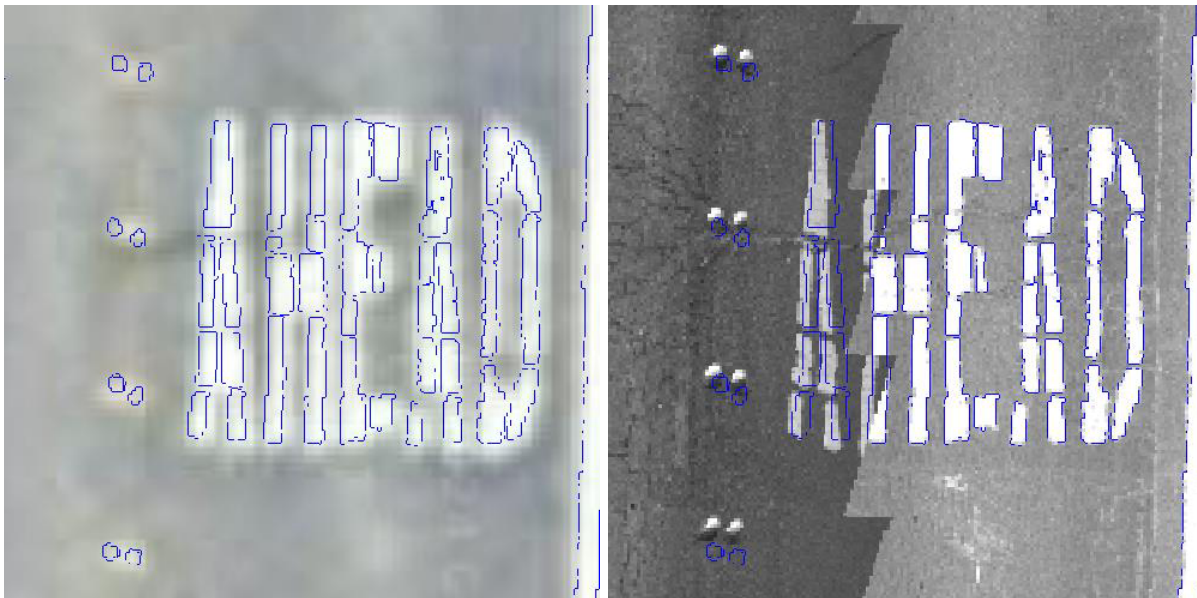


Figure 3.15: Example close-up view of orthographic mosaics illustrating minor misalignment between runs traveling in opposite directions (image on the right) and with the Google Earth imagery (image on the left). The blue line lines represent the lane marking edges detected from images traveling westbound.

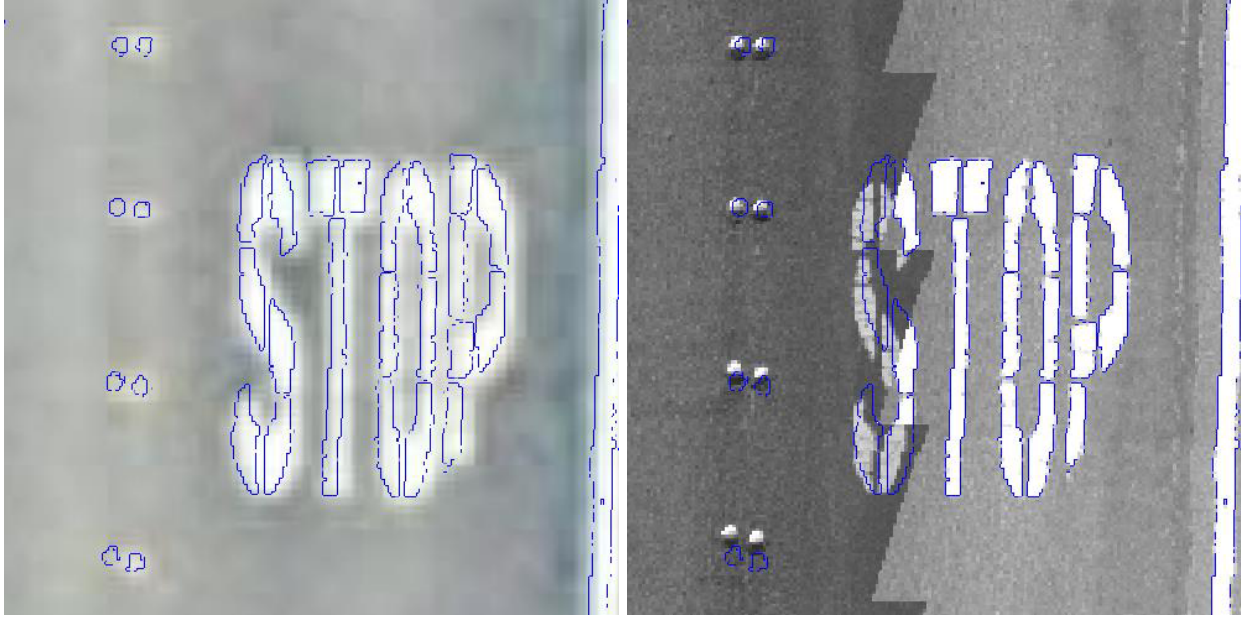


Figure 3.16: Second example close-up view of orthographic mosaics illustrating minor misalignment between runs traveling in opposite directions (image on the right) and with the Google Earth imagery (image on the left). The blue line lines represent the lane marking edges detected from images traveling westbound.

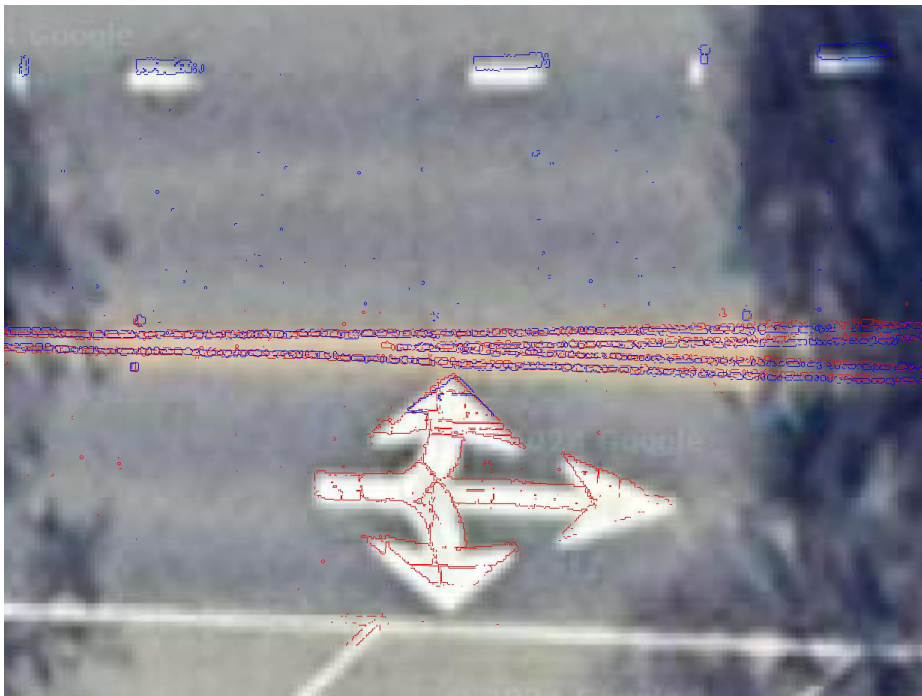


Figure 3.17: Third example close-up view (without orthographic mosaics) illustrating minor misalignment between runs traveling in opposite directions and with the Google Earth imagery. The red lines represent the lane marking edges detected from images traveling eastbound, and the blue line lines represent the lane marking edges detected from images traveling westbound.

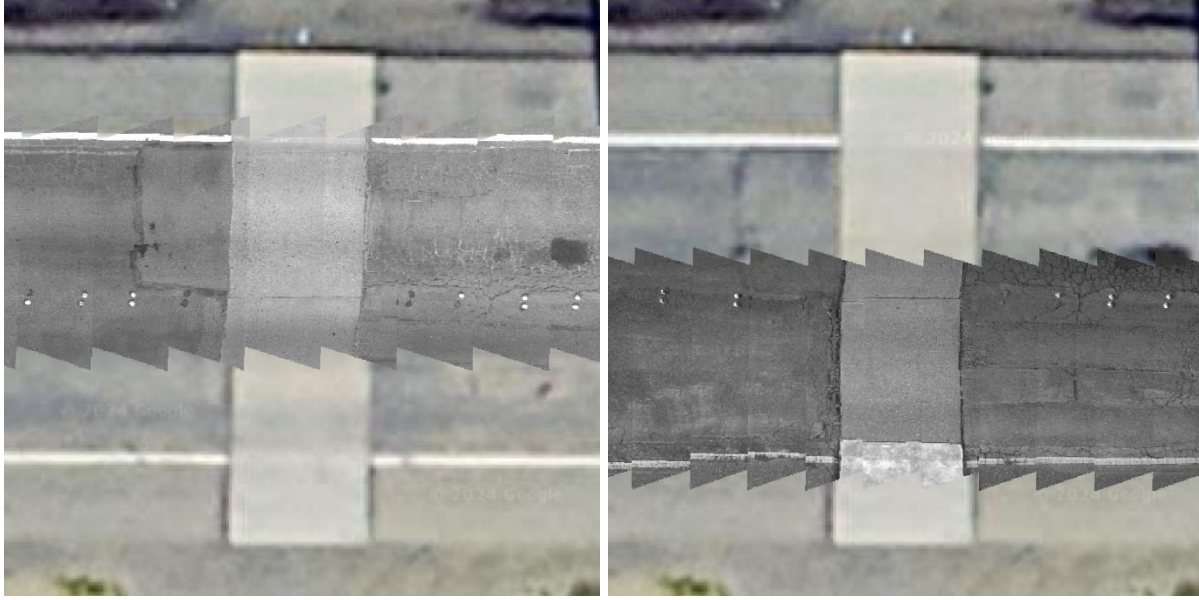


Figure 3.18: Example orthographic mosaics illustrating more noticeable longitudinal misalignment with the Google Earth imagery

Figure 3.18 shows an example with noticeable longitudinal misalignment between orthographic images and the Google Earth image. This misalignment was likely caused by vehicle bounce and/or large changes in vehicle pitch angle. The current perspective transformation parameters do not account for large changes in vehicle height (vehicle bounce), roll, and pitch. Thus, the registration error will increase at sharp curves or on bumpy roads. Based on the current results, AHMCT researchers estimate the error to be within 1 foot.

The user can adjust the image rendering resolution at the post-processing output stage. Higher resolutions tend to result in significantly larger output files, often causing higher load times and lower user responsiveness in Google Earth. AHMCT researchers have found that ArcGIS is able to handle large GeoTIFF files better than Google Earth.

Chapter 4:

Hardware Updates to Support Georeferencing Images from IR and B/W Cameras

Hardware changes

Changes to the NDE vehicle hardware were made based on the software requirements and lessons learned when operating 3D-GPR, IR cameras, and B/W cameras. Figure 4.1 shows an updated NDE vehicle system diagram. An additional RS232 connection was added between the computer and the Applanix POS system. Furthermore, the 100-Megabit Ethernet switch was upgraded to a Gigabit Ethernet switch, and a USB 3 Gigabit Ethernet adapter was also installed to connect the computer to the Gigabit Ethernet switch.

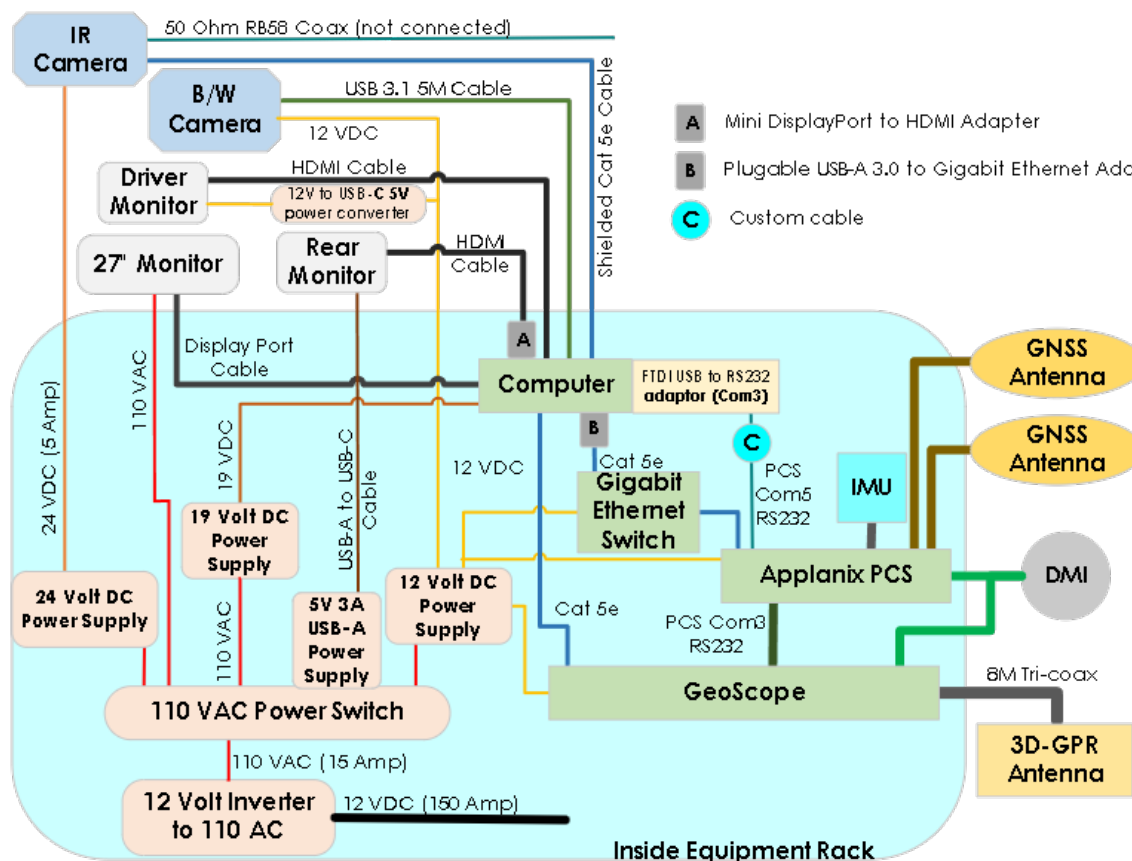


Figure 4.1: Updated NDE vehicle system wiring diagram

The RS232 serial connections have been changed. Table 4.1 summarizes the final RS232 ports settings on the NDE vehicle and Applanix computers. The 20 Hz update is for GeoScope and is based on GeoScope's recommendations. The 10 Hz Com5 rate is for IrSUITE based on the Nexco representative's setup.

Table 4.1: Serial port settings

Devices	To	RS232 Baud Rate	NMEA Message Settings
Applanix PCS COM3	GeoScope GPS input (Null modem adapter required)	115200	GPGLGA @20 Hz
Applanix PCS COM5	Computer COM3	19200	GPGLGA @10 Hz
Computer COM3 via FTDI USB-to-serial	Applanix PCS COM5	19200	GPGLGA @10 Hz

Ethernet switch upgrade

A Caltrans-approved Cisco IE1000-4T1T-LM 4-port managed industrial 100-Megabit Ethernet switch was originally installed in the previous project. The 100-Megabit Ethernet switch, which was connected to the Ethernet port of the computer, GeoScope, and Applanix PCS enables the computer to control and collect data from the GeoScope and Applanix PCS. During a pilot project, we learned that the NDE vehicle computer must have a dedicated Gigabit Ethernet link to the GeoScope to collect high-speed 3D-GPR data without any data loss. Consequently, one of the NDE vehicle computer's Gigabit Ethernet ports was rerouted to connect directly to the GeoScope's Gigabit Ethernet port. In addition, the Cisco IE1000-4T1T-LM Ethernet switch was replaced with a Gigabit Ethernet switch. The NDE vehicle computer is connected to the Gigabit Ethernet switch via a USB 3 to Gigabit Ethernet adapter made by Pluggable.

Display upgrade

A 15.6-inch 1080p high brightness display was procured to replace the original 7-inch driver display. The larger display helps the driver see the vehicle travel path history better. Figure 4.2 shows the larger upgraded display installed in the NDE vehicle.



Figure 4.2: Upgraded front vehicle display showing the vehicle trajectory and GNSS satellite availability

Applanix POS sensor offsets

The Applanix LV220 POS sensor offsets and values were evaluated, and new measurements were made to check the previous setting values. Table 4.2 and 4.3 show the updated setting values.

Table 4.2: Applanix setting values for front 3D-GPR antenna. The Front 3D-GPR center is the reference point in this table.

Descriptions	X (meter)	Y (meter)	Z (meter)
Reference point to Primary GNSS antenna	-3.94	-0.79	-1.62
Reference point to IMU	-5.29	-0.44	-1.15
Reference point to DMI	5.941	-0.86	0.593
Reference point to Auxiliary GNSS antenna	-6.46	-0.79	-1.66
GNSS Azimuth Measurement System (GAMS) vector	0.024	-2.52	0.008
DMI scale factor	1707 pulse per meter		

Table 4.3: Applanix setting values for rear 3D-GPR antenna. The rear 3D-GPR center is the reference point in this table.

Descriptions	X (meter)	Y (meter)	Z (meter)
Reference point to Primary GNSS antenna	5.046	-0.79	-2.15
Reference point to IMU	3.694	-0.44	-1.67
Reference point to DMI	3.033	-0.85	0.083
Reference point to Auxiliary GNSS antenna	2.524	-0.79	-2.16
GAMS vector	0.024	-2.52	0.008
DMI scale factor	1707 pulse per meter		

Electronics and wiring for georeferencing images from IR and B/W camera

To minimize system complexity, AHMCT researchers originally experimented with georeferencing the B/W images without hardwired time synchronization. The resulting mosaic images' longitudinal alignment error was observed to increase as vehicle speed increased due to timing errors and uncertainty between the position update time and image capture time. Thus, the final system implementation includes hardware to allow better time-tagging and synchronization with the vehicle position and orientation data.

The Applanix LV220 POS has four opto-isolated event input triggers. Detailed event input specifications are available in the Applanix POS manual. When the event input is triggered by a digital pulse, the Applanix POS system will record the event trigger time. The Applanix event input can be configured to detect and use either the rising edge or the falling edge of the digital pulse as trigger. Users can then export all event times, positions, and orientations after post-processing. The FLIR B/W camera has an opto-isolated digital output that can be configured in "ExposureActive" mode and activated using the electronic shutter of the CMOS image sensor. In this mode, by default, the digital output pulse signal's rising edge represents the beginning of the electronic shutter activation, and the falling edge represents the end of the electronic shutter activation. The pulse width time is equal to the shutter speed (exposure time). The camera can be configured to invert this signal output, such that the rising edge signals the end of the sensor exposure.

For the NDE vehicle system, the Applanix Event 1 is set to trigger on rising edge, and the FLIR B/W digital output signal is set to use an inverted ExposureActive pulse. In this scenario, the Applanix Event 1 is triggered at the end of exposure of every image. Figure 4.3 shows the wiring diagram of the connection between FLIR B/W camera and the Applanix system for event triggering. The red line represents the digital signal pulse shape to the Applanix event trigger input. Using this setup, the Applanix system will accurately timestamp every B/W image's end of exposure. After the Applanix data post-processing, all image collection times, and 3D-GPR sensor positions and orientations at the time of image collection are exported in the Applanix Smoothed Best Estimate of Trajectory (SBET) file format for the B/W camera post-processing software to import, allowing for improved mosaic rendering due to higher accuracy of position and heading information for each frame.

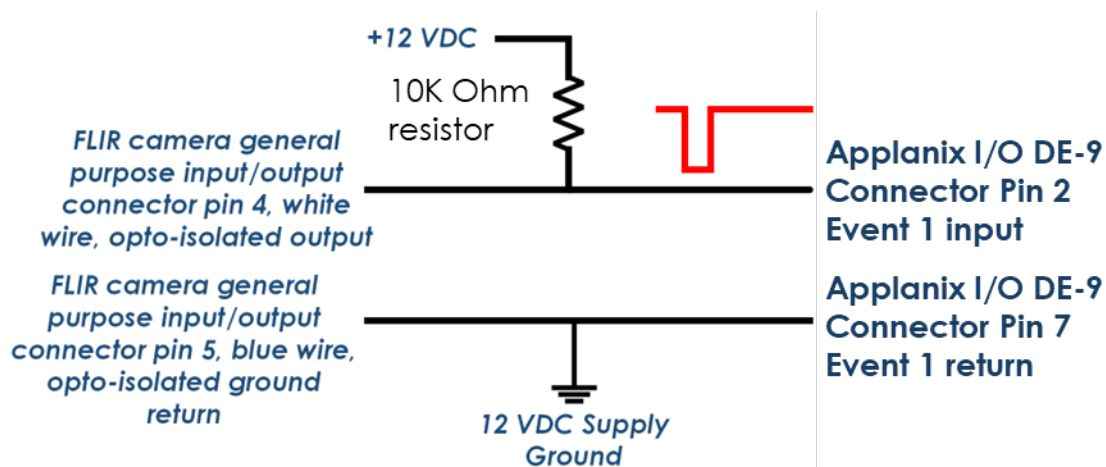


Figure 4.3: Wiring diagram of connections allowing the FLIR B/W camera to trigger Applanix events

Chapter 5:

Deployment and Implementation

Problems and issues that affected product deployment and operation

Development of a Standard Operating Procedure (SOP) would enable Caltrans' consistent application of this important technology as well as document the corresponding benefits of improved infrastructure diagnostics and maintenance. The SOP will form the implementation plan. However, more pilot projects must be completed to gain information on users' experience and expertise to develop a sound SOP.

The SOP would include:

- Best practices in identification of thermal anomalies associated with pavement and bridge deck defects.
- Recommendations for isolating anomalies and discriminate thermal anomalies from noise.
- Recommendations for data interpretation and presentation for thermal IR and GPR data sets, including ability to maximize positive identification of pavement/deck defects.

Recommended solutions to noted problems and issues

More pilot projects on using the IR camera are needed to gain experience in data collection and analysis. Extensive real project experience is a prerequisite for developing a sound SOP and recommendations for IR anomaly identification. Careful documentation of lessons learned is vital for continuing successful future deployment and maintaining institutional knowledge for the next generation of users.

Issues expected to affect full implementation

Additional pilot projects should be conducted to gain experience for data collection best practices, interpretation of data, and expertise development. After that, the developed user experiences and expertise can then be documented systematically in SOP and best practices documentation.

Other considerations for reaching full product deployment & optimal operation

Equipment issues

None

Operational issues

Developing an SOP for collecting and processing georeferenced thermal IR data is the next major challenge. More research and pilot projects are needed to gain the necessary know-how for SOP development.

Policy issues

Full deployment will entail closer collaboration with Materials Engineering and Testing Services, Structures Maintenance & Investigations, and the Division of Maintenance Pavement Program. Appropriate roles, responsibilities, and resourcing will need to be developed to integrate these tools into inspection practice. Future full system deployment may impact reorganization plans within the Division of Engineering Services.

Chapter 6:

Conclusions and Future Research

Key contributions of this research project included:

- Reviewed and selected IrSUITE IR camera data collection and analysis software for pavement delamination and debonding.
- Changed the Caltrans NDE vehicle to support the installation and operation of the IrSUITE software as well as georeferencing of IR camera data.
- Facilitated IrSUITE training for Caltrans users.
- Developed a Python program to update IrSUITE position log file with post-processed Applanix POS position coordinates.
- Upgraded the Caltrans NDE vehicle hardware based on the lessons learned from these projects.
- Modified B/W camera wiring to the Applanix system to support high-accuracy georeferencing of B/W images.
- Developed and tested B/W camera data collection and post-processing software.
 - Implemented high-accuracy georeferencing of B/W images.
 - Implemented a glare reduction process for B/W images.
 - Implemented an MP4 video exporting feature.
 - Implemented perspective view to orthographic view image transformation.
 - Implemented a GeoTIFF export feature.

The results of this project enable Caltrans to start using thermal IR camera for early identification of shallow-seated deterioration in pavements and bridge decks. The B/W imagery could help users better identify real and false anomalies in the 3D-GPR and IR data. This research directly aligns with Caltrans' Strategic Goal of Stewardship and Efficiency as it supports consistent application of thermal IR data collection and processing for improved infrastructure inspection and maintenance. Furthermore, this research allows thermal IR data collection from a moving vehicle, keeping workers off the pavement to improve safety. Currently no other DOT possesses the unique combined capability of mobile 3D GPR and thermal IR imaging. Thus, this

research contributes to Caltrans' Organizational Excellence strategic goal by continuing and enhancing Caltrans' national leadership in the application of NDE methods for highway infrastructure.

Future work

The findings from this research suggest several avenues for future research and development.

1. This research resulted in an NDE vehicle with 3D-GPR, IR camera, and B/W camera for Caltrans to conduct various pilot projects. Caltrans has completed multiple projects with the 3D-GPR system. However, Caltrans has only conducted limited projects using the IR camera. More pilot projects using the IR camera are needed to gain experience in data collection and analysis. Real project experience is a prerequisite for developing a sound SOP and recommendations for IR anomaly identification. Careful documentation of lessons learned is vital for continuing successful future deployment and to maintain institutional knowledge for the next generation of users.
2. Further development and testing are needed to enhance the B/W camera post-processing software to support multi-processing to reduce processing time and enable breaking down a single, large GeoTIFF image into multiple, smaller GeoTIFF images.
3. Currently, users have to review each thermal image manually to identify possible anomalies (defects in the pavement). This manual task is time consuming and labor intensive. Software automation, possibly using Machine Learning technologies, could reduce time and labor to post-process the data and identify possible anomalies for users to review for quality control and quality assurance. However, application of Machine Learning requires a large, known good dataset and would leverage available research and resources. More pilot IR camera projects must be completed first to gather a good Machine Learning training dataset.
4. Evaluate the use of 24MP B/W camera with a polarized filter.

References

- [1] K. Yen and T. Lasky, "Research to Integrate Color and Thermal Imaging IR Cameras with Caltrans 3D-GPR and GNSS/INS System," CA20-3608, Apr. 2020. [Online]. Available: <https://ahmct.ucdavis.edu/sites/g/files/dgvnsk8581/files/inline-files/UCD-ARR-20-04-30-01.pdf>
- [2] Z. Shen, C. Cheng, R. Na, and Z. Shang, "To Automate Detecting, Quantifying and Mapping of Delamination via Arial Thermography," no. SPRP1(20) M109, Dec. 2020, [Online]. Available: <https://rosap.nhl.bts.gov/view/dot/55858>
- [3] C. Cheng, Z. Shang, and Z. Shen, "Automatic delamination segmentation for bridge deck based on encoder-decoder deep learning through UAV-based thermography," *NDT E Int.*, vol. 116, p. 102341, Dec. 2020, doi: 10.1016/j.ndteint.2020.102341.